AMERICAN SOCIETY FOR MICROBIOLOGY | mBio

Check for updates

| Genomics and Proteomics | Research Article

Comparative genomics and stable isotope analysis reveal the saprotrophic-pathogenic lifestyle of a neotropical fungus

Luiz Marcelo Ribeiro Tomé,[1] Gabriel Quintanilha-Peixoto,[1] Diogo Henrique Costa-Rezende,[2] Carlos A. Salvador-Montoya,[3,4,5] Domingos Cardoso,[6,7] Daniel S. Araújo,[8] Jorge Marcelo Freitas,[9] Gabriela Bielefeld Nardoto,[9] Genivaldo Alves-Silva,[3] Elisandro Ricardo Drechsler-Santos,[3] Aristóteles Góes-Neto[1]

AUTHOR AFFILIATIONS See affiliation list on p. 14.

ABSTRACT In terrestrial forested ecosystems, fungi may interact with trees in at least three distinct ways: (i) associated with roots as symbionts; (ii) as pathogens in roots, trunks, leaves, flowers, and fruits; or (iii) decomposing dead tree tissues on soil or even on dead tissues in living trees. Distinguishing the latter two nutrition modes is rather difficult in Hymenochaetaceae (Basidiomycota) species. Herein, we have used an integrative approach of comparative genomics, stable isotopes, host tree association, and bioclimatic data to investigate the lifestyle ecology of the scarcely known neotropical genus *Phellinotus*, focusing on the unique species *Phellinotus piptadeniae*. This species is strongly associated with living *Piptadenia gonoacantha* (Fabaceae) trees in the Atlantic Forest domain on a relatively high precipitation gradient. Phylogenomics resolved *P. piptadeniae* in a clade that also includes both plant pathogens and typical wood saprotrophs. Furthermore, both genome-predicted Carbohydrate-Active Enzymes (CAZy) and stable isotopes ($\delta^{13}C$ and $\delta^{15}N$) revealed a rather flexible lifestyle for the species. Altogether, our findings suggest that *P. piptadeniae* has been undergoing a pathotrophic specialization in a particular tree species while maintaining all the metabolic repertoire of a wood saprothroph.

IMPORTANCE This is the first genomic description for *Phellinotus piptadeniae*. This basidiomycete is found across a broad range of climates and ecosystems in South America, including regions threatened by extensive agriculture. This fungus is also relevant considering its pathotrophic-saprotrophic association with *Piptadenia goanocantha*, which we began to understand with these new results that locate this species among biotrophic and necrotrophic fungi.

KEYWORDS fungus-plant interactions, Hymenochaetaceae, Fabaceae, CAZy, C13/N15 stable isotopes

The ability to thrive in a living plant host is widespread in pathogenic and symbiotic fungi. A wide range of relationships can be described among the plant-fungal interactions. Fungi can be classified as biotrophic when they derive energy from living cells; necrotrophic, when energy is obtained from killed cells (they invade and kill plant tissue rapidly and then live saprotrophically on the dead remains); or hemibiotrophic, when they engage in an initial biotrophic phase followed by necrotrophy (1). Fungal pathogens attacking wood can be classified as heart-rot fungi, which are specialized in decomposing the heartwood of trees, with the colonization and decay process beginning while the host is alive. Otherwise, the decay may occur on sapwood, or the infection may advance from heartwood to sapwood (2).

The understanding of fungal symbiotic interactions and mechanisms involved in organic matter conversion are of high interest in both mycology and biotechnology.

Invited Editor David S. Hibbett, Clark University, Worcester, Massachusetts, USA

Editor Alexandre Alanio, Institut Pasteur, Paris, France

Address correspondence to Aristóteles Góes-Neto, arigoesneto@icb.ufmg.br.

Luiz Marcelo Ribeiro Tomé and Gabriel Quintanilha-Peixoto contributed equally to this article. The order of co-first authors was determined based on their contributions to the experiments and bioinformatics analyses.

The authors declare no conflict of interest.

See the funding table on p. 15.

Received 3 June 2024
Accepted 20 June 2024
Published 16 July 2024

Using comparative genomics is a viable approach to this theme (3). Various studies show that different mechanisms could be related to the trophic mode of fungi, such as the presence and abundance of gene families related to the decaying of lignocellulosic material (4, 5). Furthermore, different nutrition modes in fungi can be correlated to different stable isotope signatures (such as carbon and nitrogen), allowing the distinguishing of whether nutrition is acquired from dead organic matter, or a living symbiont (6–9).

Hymenochaetales fungi exhibit a wide range of lifestyles, such as saprotrophic, mycorrhizic, bryophyllic, and plant pathotrophic (9, 10). A deep investigation of trophic modes in Hymenochaetales, based on stable isotope analyses, has revealed a greater diversity of trophic modes in this order than previously assumed. The species in Hymenochaetales can be broadly classified as saprotrophic (lignicolous species), or in other two groups of biotrophic taxa (although not necessarily parasitic), one composed mainly of ectomycorrhizae, and the second including ectomycorrhizae, saprotrophs, and briophyllous fungi (9). The family Hymenochaetaceae, the most representative in the order, encompasses several plant pathogens (11, 12). While these fungi frequently decompose dead portions of the trees (heart rot), cases in which some of these hymenochaetoid fungi attack the living and defense-active sapwood are also reported (2). Thus, it is debatable whether these pathogens would have isotope signatures closer to the saprotrophic, or one of the biotrophic clusters recovered by Korotkin et al. (9). In the same way, understanding whether the gene profile related to lignocellulose decay of those fungi tends to be more similar to non-pathogenic species (exclusively saprotrophs) or other trophic modes is also an open question.

The exclusively neotropical hymenochaetaceous species *Phellinotus piptadeniae* (Teixeira) Drechsler-Santos & Robledo has been described with an intriguing pathogenic mode (13–16). Recently, Salvador-Montoya et al. (2022) (14) refined the taxonomic concept of this species based on its morphology, distribution, and host association. Accordingly, the perennial basidiomata of *P. piptadeniae* are found on living trees of the legume species *Piptadenia gonoacantha* (Mart.) J.F. Macbr. (recurrent host), as well as other species of Fabaceae and Myrtaceae (14, 16). Based on the studies of Elias et al. (16) and Salvador-Montoya et al. (14), several collections of basidiomata of *P. piptadeniae* are recorded, mainly on living trees of *P. gonoacantha*, usually found on high branches of the trees, which eventually are aborted (break and fall off the tree), and rarely on the trunk, but also on dead branches of living trees.

To clarify plant pathogenic interactions in this ecologically interesting species, *Phellinotus piptadeniae*, its complete genome was newly sequenced, assembled, and annotated. We subjected this new genome to a phylogenomic and comparative genomics approach with other publicly available, high-quality assembled genomes of Hymenochaetales. Moreover, a molecular clock analysis was performed to evaluate whether the current taxonomic concept of the species comprises a hidden diversity. Finally, stable isotope signature (C13 and N15) of the species was accessed for the first time and compared with fungi from different trophic modes in Basidiomycota. The findings of our study reveal new insights, suggesting that *P. piptadeniae* may be regarded as a significant fungal pathogen within South American tropical forest biomes.

RESULTS

Phellinotus piptadeniae host and climate range

Across its full distribution range from northern Brazil to central Uruguay, *Phellinotus piptadeniae* has shown a higher ecological preference for the more humid regions of mostly the Atlantic Forest and Pampa phytogeographic domains (Fig. 1A and B). Annual precipitation in those regions ranges from around 1,200 to 1,500 mm (Fig. 1B). A few collection sites in the Caatinga seasonally dry woodlands of northeastern Brazil were also detected, where this fungal species grows in sites with less than 500 mm annual precipitation. All records in the savannas of the Cerrado and Pampa grasslands also came from relatively wet sites (Fig. 1B). *Phellinotus piptadeniae* basidiomata

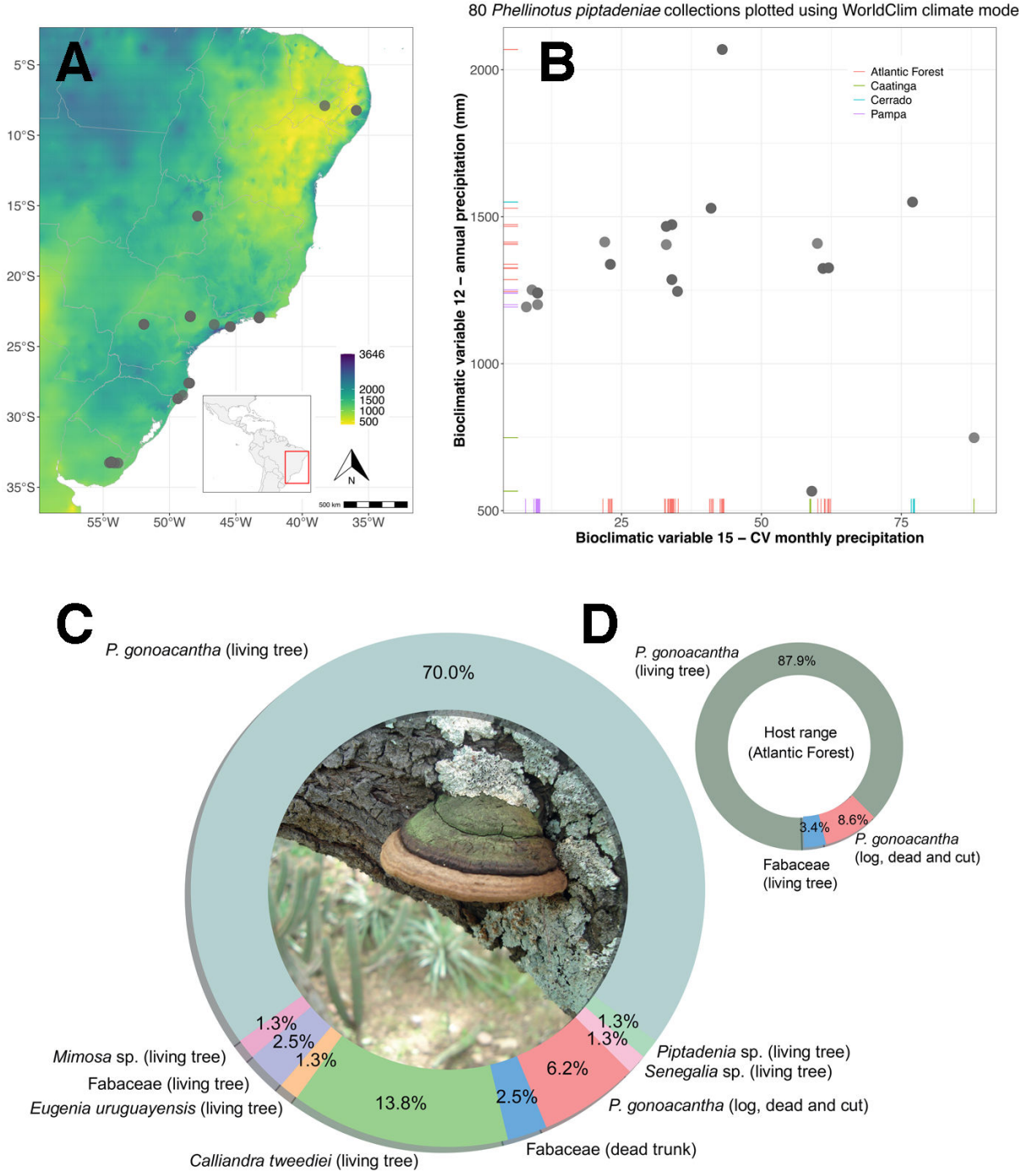

FIG 1 Geographical range of *Phellinotus piptadeniae* across a precipitation gradient (A) as retrieved from the WorldClim bioclimatic variable 12 (17). The species shows a higher ecological preference for wetter regions, mostly in the Atlantic Forest and Pampa phytogeographic domains, except for a few collections in the Caatinga (B). Total host range of *Phellinotus piptadeniae*, accounting for Brazil and Uruguay specimens (C) and across the Atlantic Forest only (D). Photo of *Phellinotus piptadeniae* in detail by E.R. Drechsler-Santos.

were predominantly found on *Piptadenia gonoacantha* living trees (Fabaceae). Fungal samples were also found growing on the legume *Calliandra tweediei* Benth. and *Eugenia uruguayensis* Cambess. (Myrtaceae) besides other unidentified species of the legume genera *Mimosa*, *Piptadenia*, and *Senegalia* (Fig. 1C and D; Table S1 [available at https://github.com/LBMCF/phepip_isotopes]).

Phellinotus piptadeniae genome sequencing, assembly, and annotation metrics

Sequencing on the Illumina HiSeq 2500 platform generated 28,672,142 paired-end short reads, corresponding to 3,784,150,188 bases. Through sequencing on the Oxford Nanopore Technologies' MinION, we obtained 409,847 long reads, corresponding to 772,618,969 bases. Using the MaSuRCA-Purge_dups assembly pipeline, we obtained an assembly with 418 contigs, 32,966,471 bp in length, in which the largest contig was 813,870 bp long, N50 of 203,956 bp, L50 of 45, and GC content of 47.73%.

The genome of *P. piptadeniae* has 9,771 protein-coding genes. Sequencing depths of 114× and 23× were obtained on the HiSeq 2500 and MinION platforms, respectively. The newly assembled genome possesses 95.6% of the orthologous genes searched through the BUSCO analysis. Among those orthologous genes, 93.3% were classified as single copy, 2.3% as duplicated, 1% as fragmented, and 3.4% as missing (see Fig. S1 at https://github.com/LBMCF/phepip_isotopes).

Comparative genomics and phylogenomics of Hymenochaetales

The dated phylogenomic tree (Fig. 2) suggests that *P. piptadeniae* diverged from its MRCA around 2 million years ago (Mya), in the Pleistocene. Our dating analysis could not obtain enough resolution to separate the clade containing *P. piptadeniae*, *Sanghuangporus*, *Inonotus*, *F. mediterranea*, and *P. igniarius* (Fig. 2). Nonetheless, before the dating analysis, we described that *P. piptadeniae* shares its MRCA with the genera *Sanghuangporus* and *Inonotus*, in a clade that diverged from *F. mediterranea* and *P. igniarius* (Fig. 2, detail box). All clades have a branch support of 100% (see Fig. S2 at https://github.com/LBMCF/phepip_isotopes), except for the clade including *P. noxium* FFPRI411160 and *P. noxium*

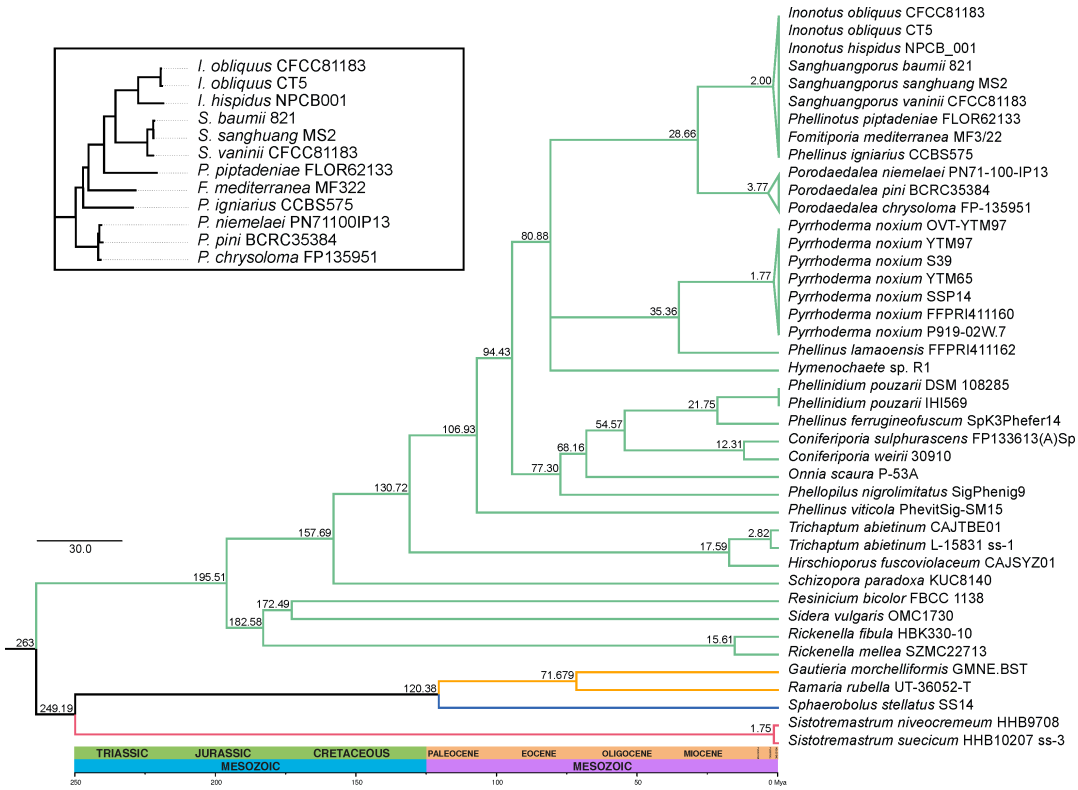

FIG 2 Phylogenomic dated tree showing the placement of *Phellinotus piptadeniae* in the context of the lineages *Hymenochaetales* (light green branches), *Gomphales* (orange), *Trechisporales* (magenta), and *Geastrales* (blue). The tree was calibrated using the MRCA of *Hymenochaetales* and *Trechisporales* (243 Mya), and the MRCA of *Phellinus igniarius* and *Fomitiporia mediterranea* (2.003 Mya). Other nodes were calculated using the least-squares method of IQTree. Clade separation containing *P. piptadeniae*, without time estimates, is shown in the detail box.

P91902W7, with a support of 96%. The full list of genomes with respective accession codes is available in Table S2 (available at https://github.com/LBMCF/phepip_isotopes).

The genome size in Hymenochaetales (i.e., excluding the outgroup) ranged from 28.45 to 67.25 Mbp (mean = 41.30 Mbp, median = 37.10 Mbp) (Fig. 3A and B). The genome of *P. piptadeniae* is within the range expected for the order, and phylogenetically in a clade that contains species with similar genome sizes. The same is observed for the GC content, which ranged from 40.83% to 52.43% (mean = 46.95%, median = 47.99%), showing that the genome of *P. piptadeniae* has GC content close to both the expected mean and median, and the species is phylogenetically grouped with genomes with similar GC content (Fig. 3A through C). We also evaluated the completeness of the genome used in phylogenetic analysis (obtained from JGI and NCBI) for single-copy orthologous gene content. The completeness of genomes belonging to Hymenochaetales ranged from 77.4% to 97.6% (mean = 91.84%, median = 93.9%) (Fig. 3A through D). And, again, the genome of *P. piptadeniae* exhibits completeness greater than both mean and median for Hymenochaetales, demonstrating the quality of the genome generated in our study.

We obtained a pangenome of the selected species through ortholog family determination with OrthoFinder (Fig. 4). Orthogroup determination was performed as seen in Petersen et al. (18). In this ortholog distribution, a total of 27,834 orthogroups were obtained, out of which 2,099 orthogroups were designated as the core pangenome (present in all assemblies) and 1,834 orthogroups are part of the softcore pangenome (≥95% of the genomes). The variable part of the pangenome was composed of the

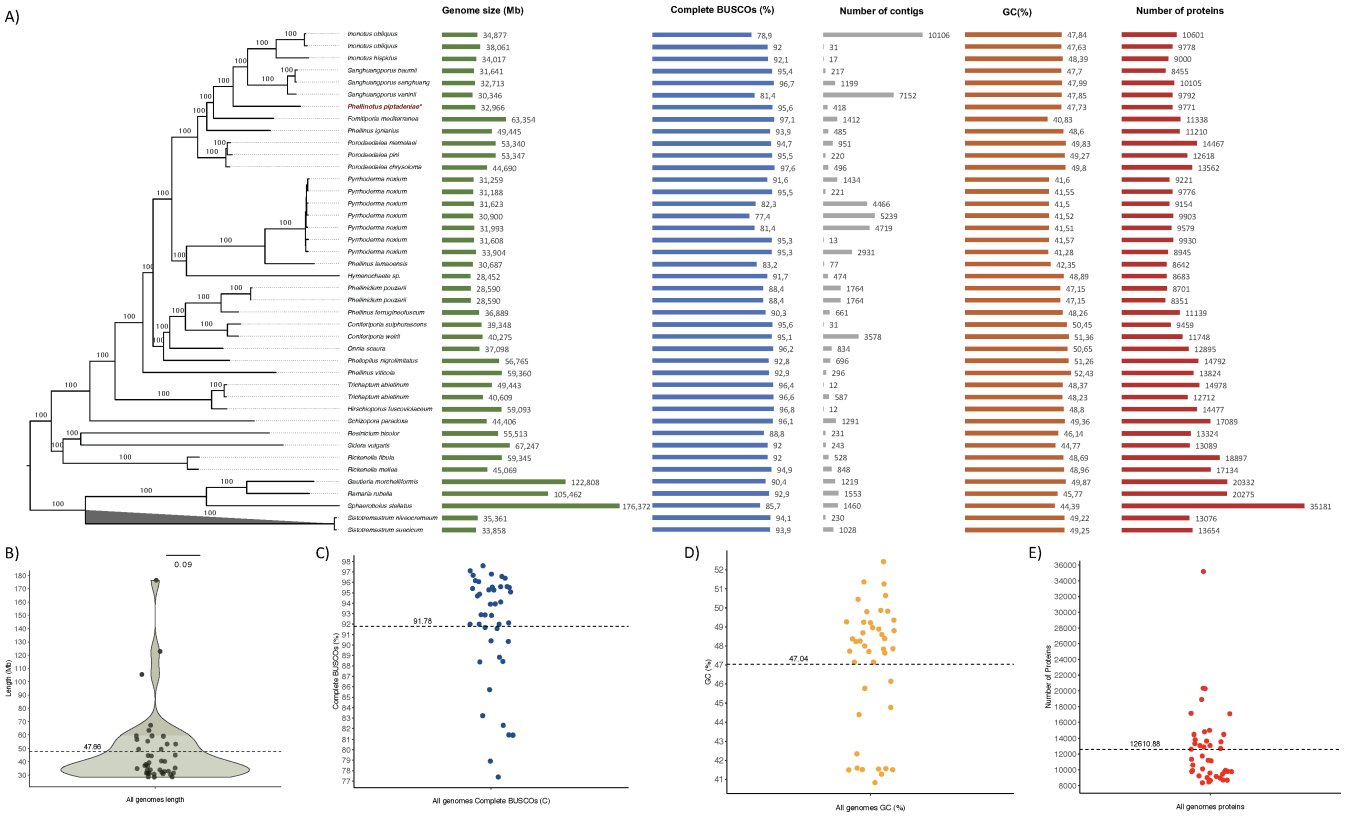

FIG 3 (A) Hymenochaetales maximum likelihood (ML) phylogeny plotted with data on genome size, gene completeness (BUSCO analysis), number of contigs, GC content, and number of proteins, including the genome of *Phellinotus piptadeniae*, 36 genomes belonging to other Hymenochaetales species, and five genomes belonging to the outgroup. (B) Dot and violin plots show genome size variation for Hymenochaetales and highlight the mean for the analyzed metric. (C) The dot plot shows genome completeness inferred using BUSCO. (D) The dot plot shows the variation of GC content for Hymenochaetales and highlights the average for the analyzed metric. (E) The dot plot shows the variation of predicted protein content for Hymenochaetales and highlights the average for the analyzed metric.

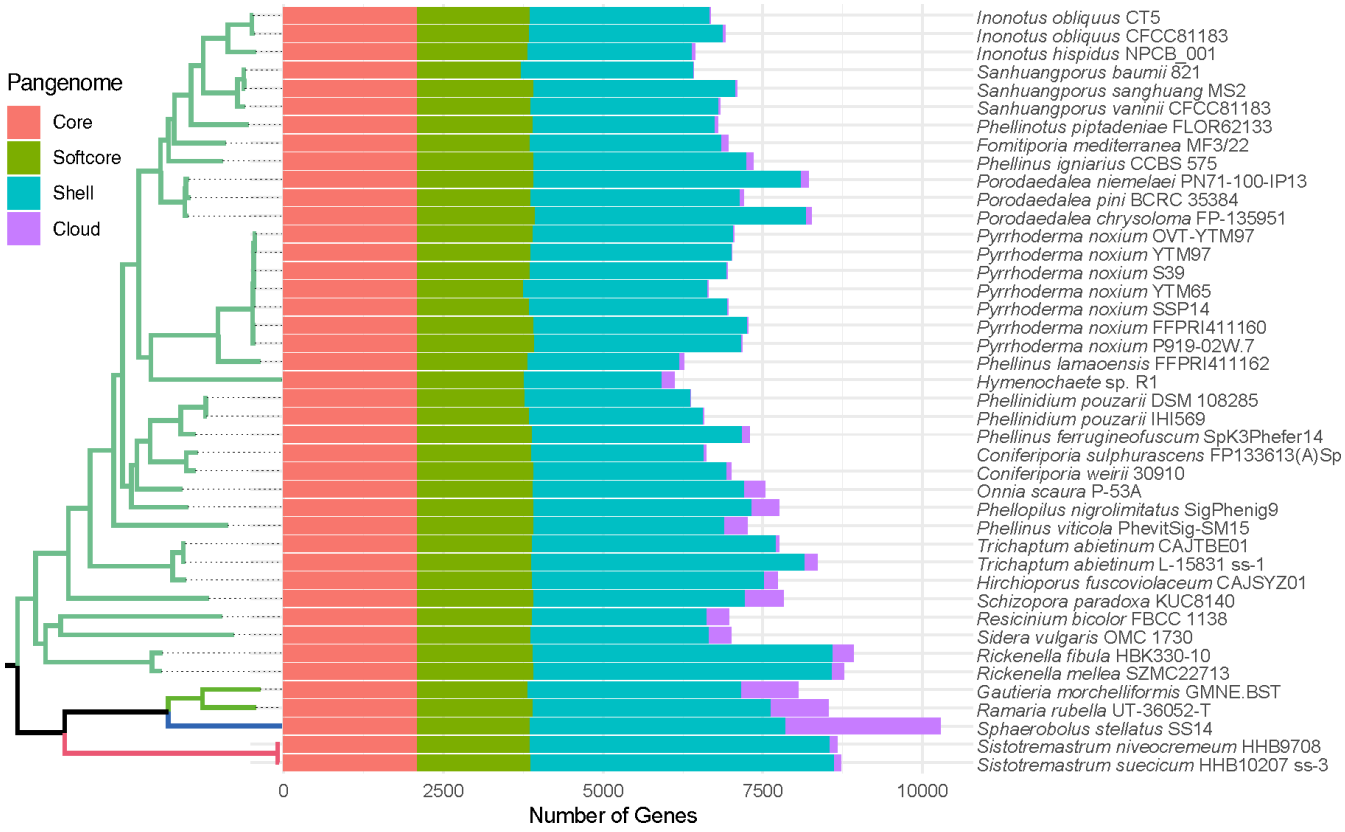

FIG 4 Pangenome distribution determined by OrthoFinder. Pangenome classes are as determined in Petersen et al. (18).

shell (<95%, >2% of the assemblies), composed of 14,924 orthogroups, and the cloud pangenome (genome-exclusive orthogroups), composed of 8,977 orthogroups spread throughout assemblies. A full table with the numbers used in Fig. 4 is available in Table S3 (available at https://github.com/LBMCF/phepip_isotopes).

Regarding its genome structure, *P. piptadeniae* fits the average genome length and GC content. Relevant gene deletions could not be detected in this species either, in which 51 ortholog families were detected as species-exclusive (cloud pangenome, Fig. 4; Tables S3 and S4 [available at https://github.com/LBMCF/phepip_isotopes]). Over 70% of these species-exclusive ortholog families have disordered regions (36). In half of these families (18), all orthologs have been categorized as effectors, plus another 17 in which most or some orthologs were detected as effectors. Protein domains could only be identified in nine species-exclusive ortholog families. These include Hsp70 chaperones, membrane transporters, secondary metabolite and siderophore biosynthesis, DNA repair, proteolysis, and detoxification.

Stable isotope and CAZy clustering analyses reveal a flexible lifestyle in *P. piptadeniae*

A total of nine *Phellinotus piptadeniae* basidiomata were analyzed for $\delta^{13}C$ and $\delta^{15}N$ stable isotopes, deriving from distinct dead branches of living *Piptadenia gonoachanta* trees jointly with their leaves (Fig. 5A and B). The dead branches of the living trees were still completely attached to the trunk or detached from the trunk, but not on the soil. As expected, the leaves exhibited a significantly lower $\delta^{13}C$ ($P < 0.001$, Fig. 5A) and a significantly higher $\delta^{15}N$ ($P < 0.001$) than both wood from dead branches and fungal basidiomata (Fig. 5B). Regardless of sample origin (attached or detached from tree trunks), both $\delta^{13}C$ (Fig. 5A) and $\delta^{15}N$ (Fig. 5B) patterns were very similar, in which values were situated between tree leaves and fungal basidiomata values. Although the $\delta^{15}N$

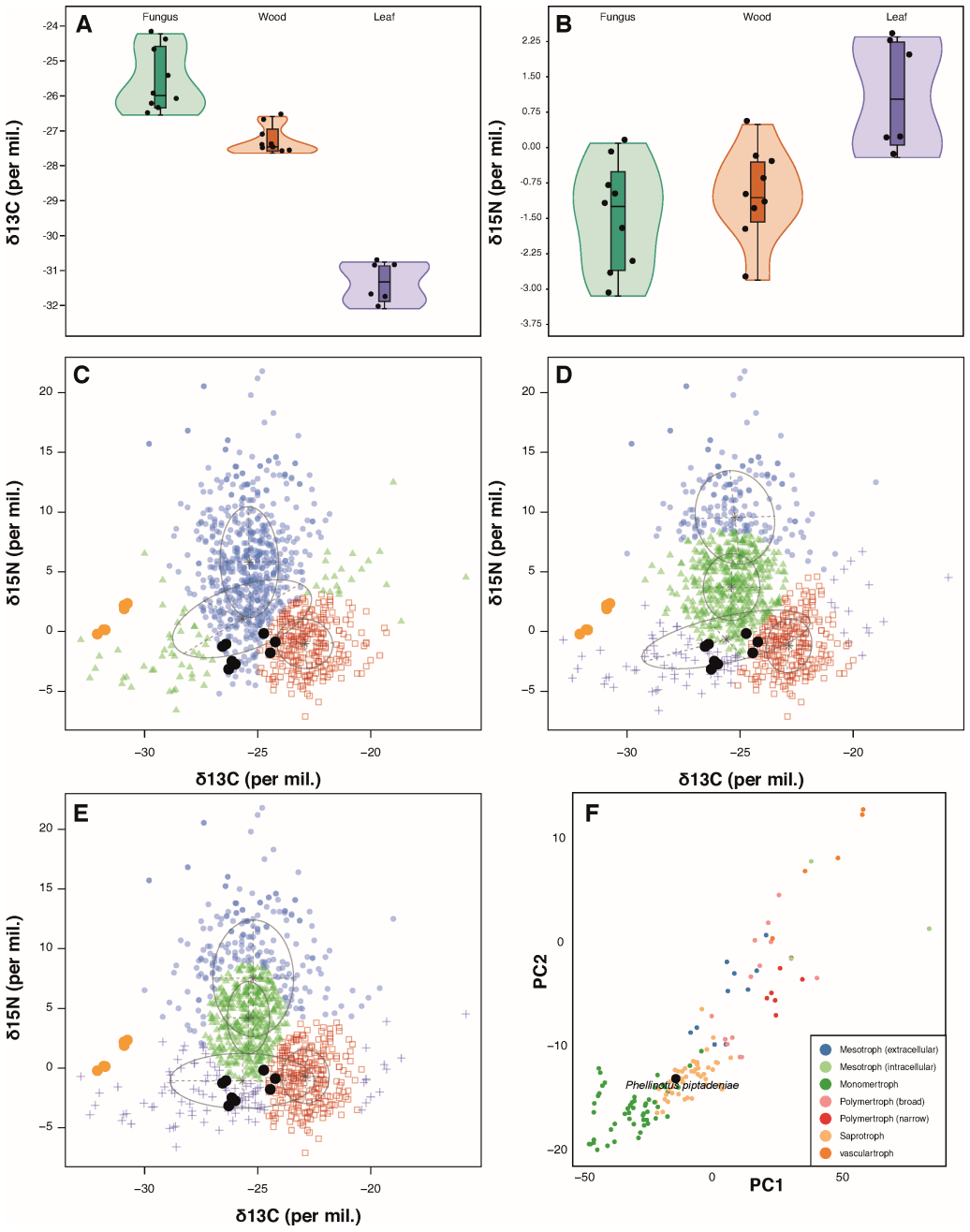

FIG 5 (A-B) $\delta^{13}C$ and $\delta^{15}N$ stable isotope patterns in *P. piptadeniae* basidiomata (fungus), *P. gonoachanta* branches (wood), and leaves (leaf) samples. (A) Values of $\delta^{13}C$ (per mil.). (B) Values of $\delta^{15}N$ (per mil.). (C-E) *Mclust* analysis of *P. gonoacantha* leaves (orange) and *P. piptadeniae* (black) samples from this study and 957 other samples compiled by Korotkin et al. (9). (C) *Mclust* with the VVV model and three components. (D) *Mclust* with the VEV model and four components. (E) *Mclust* with the VVI model and four components. (F) Catastrophy clustering of the CAZy composition of 99 fungal species compiled by Zhao et al. (4) plus *P. piptadeniae* (highlighted). Full cluster descriptions are available in Tables S5 and S6 (Fig. 5A through E), Fig. S3; Table S7.

of fungal basidiomata and wood samples were quite similar (and thus not statistically different) (Fig. 5B), their $\delta^{13}C$ values were distinct, with fungal basidiomata exhibiting higher and statistically significant ($P < 0.001$) values than tree wood (Fig. 5A).

In their study, Korotkin et al. (9) applied three *Mclust* models to separate isotope data from fungal samples; VVI (diagonal, varying volume, and shape), VEV (ellipsoidal, equal

shape), and VVV (ellipsoidal, varying volume, shape, and orientation). The fitting model presented in Fig. 5A (VVV model with three components) appears to be too simplistic to reflect the niche diversity in the samples, while the models presented in Fig. 5B and C achieved a better resolution.

Mclust with the VVV model and three components. Cluster 1 (circles) contains 7/9 *P. piptadeniae* samples. Cluster 2 (squares) includes 2/9 *P. piptadeniae* samples. Cluster 3 (triangles) contains all leaf samples. (D) *Mclust* with the VEV model and four components. Cluster 1 (circles) does not contain any samples from this study. Cluster 2 (squares) includes 2/9 *P. piptadeniae* samples. Cluster 3 (triangles) 3/9 *P. piptadeniae* samples. Cluster 4 (crosses) contains all leaf samples and 4/9 *P. piptadeniae* samples. (E) *Mclust* with the VVI model and 4 components. Cluster 1 (circles) does not contain any samples from this study. Cluster 2 (squares) includes 2/9 *P. piptadeniae* samples. Cluster 3 (triangles) 2/9 *P. piptadeniae* samples. Cluster 4 (crosses) contains all leaf samples and 5/9 *P. piptadeniae* samples. (F) Catastrophy clustering of the CAZy composition of 99 fungal species compiled by Zhao et al. (4) plus *P. piptadeniae* (highlighted). Full cluster descriptions are available in Tables S5 and S6 (Fig. 5A through E), Fig. S3; Table S7 (Fig. 5F) (all available at https://github.com/LBMCF/phepip_isotopes).

The clustering pattern for the *P. piptadeniae* samples is practically identical in Fig. 5B and C, with just one sample belonging to Cluster 3 with the VEV model and switching to Cluster 4 with the VVI model. Taking VVI as an example of the *P. piptadeniae* samples clustering, our nine fungal samples were divided into Cluster 2 (squares—two samples) composed of 76.49% saprotrophic fungi; Cluster 3 (triangles—two samples) composed of 62.48% ectomycorrhizal samples and 25.33% bryophilous Hymenochaetales; and Cluster 4 (crosses—5 samples) composed of 40% bryophilous Hymenochaetales, 9.27% saprotrophic, and 5.9% ectomycorrhizal fungi (Table S5 [available at https://github.com/LBMCF/phepip_isotopes]). Kruskal-Wallis results and subsequent Dunn test strongly support $\delta^{15}N$ and $\delta^{13}C$ stable isotope mean differences between each of the recovered clusters (Table 1). Subsequently, we tested whether *P. piptadeniae* in cluster 1 (best-fit model) has stable isotope values similar to those of known saprotrophic, ECM (ectomycorrhizal), bryophilous Hymenochaetales, NS-NE (neither saprotrophic nor ectomycorrhizal), and AUTO (autotrophic) taxa (Table 2). The latter category includes the moss species *Dicranum scoparium*, a control for the original analysis, and leaf samples from *Piptadenia gonoacantha,* as a control for our analysis.

A CAZy-based classification predicted *P. piptadeniae*, as well as all other Hymenochaetales and most other neighboring clades as saprotrophs (Fig. 4D and 6). Nonetheless, as explained by the authors, all trophic modes with a score higher than 0.8 are relevant, which then classifies *P. piptadeniae* and many neighboring genomes as possible Monomertrophs, which Hane et al. (19) describe as either symbionts or biotrophs. Notable exceptions are *F. mediterranea*, with a Monomertroph score of 0.790, and *Onnia scaura*, which presented an outlier profile and, thus, should not be considered.

TABLE 1 Comparison of trophic cluster assignments by *Mclust* to test differences in the sampling utilizing Kruskal-Wallis and Dunn tests[a]

Test	Comparison	$\delta^{15}N$	$\delta^{13}C$
Kruskal-Wallis	All clusters	Chi-square = 719.12	Chi-square = 480.24
		df = 3	df = 3
		$P < 0.00001$	$P < 0.00001$
Dunn	Cluster 1 vs cluster 3	$P < 0.0001$	$P < 0.0001$
	Cluster 1 vs cluster 2	$P < 0.0001$	$P < 0.0001$
	Cluster 2 vs cluster 3	$P < 0.0001$	$P < 0.0001$

[a]Stable isotope data from the compilation of Korotkin et al. (9) and data generated herein for *P. piptadeniae* (Table S6).

TABLE 2 Comparison of stable isotope results to test statistical differences between trophic clusters and trophic states using Kruskal-Wallis and Dunn tests[a]

Test	Trophic comparison	$\delta^{15}N$	$\delta^{13}C$
Kruskal-Wallis	*P. piptadeniae*; ECM; SAP; NS-NE; "unknown"	Chi-square = 404.18 df = 5 $P < 0.00001$	Chi-square = 464.13 df = 5 $P < 0.00001$
Dunn	*P. piptadeniae vs* AUTO	$P = 0.2145$	$P = 0.0059$
	P. piptadeniae vs ECM	$P < 0.0001$	$P = 0.3575$
	P. piptadeniae vs NS-NE	$P < 0.0001$	$P = 0.3495$
	P. piptadeniae vs SAP	$P = 0.1717$	$P < 0.0001$
	P. piptadeniae vs "Unknown"	$P = 0.0918$	$P = 0.3903$

[a]ECM = ectomycorrhizal; NS-NE = neither saprotrophic nor ectomycorrhizal (the other biotrophic ones); SAP = saprotrophic; AUTO = Autotrophic. Stable isotope data from the compilation of Korotkin et al. (9) and data generated herein for *P. piptadeniae* (Table S5).

DISCUSSION

The combination of genomics, stable isotope analyses, host tree association, and bioclimatic data has revealed more details of the interaction of *Phellinotus piptadeniae* and its main host, *Piptadenia gonoacantha* (Fig. 1C and D). Overall, we verified that the trophic mode of *P. piptadeniae* involves traits of biotrophy added to its previously known saprotrophic lifestyle. This could be a determinant of its host specificity and interaction with plant hosts.

The entire genus *Phellinotus* predominately occurs in the South American seasonally dry tropical forest (SDTF) biome (20), where each species often occurs associated with disjunct SDTF areas (13, 14). While also occurring in drier settings, *P. piptadeniae* seems to have deviated from the ancestral ecological niche of the genus to thrive in more humid settings of the Atlantic Forest, Pampa, and Cerrado phytogeographic domains (Fig. 1A and B). Whether the successful ecological adaptation of *P. piptadeniae* into these settings was enabled by the evolution of its flexible lifestyle, involving both the saprotrophy and the herein-described pathotrophic specialization, remains an open question.

Insights into the trophic mode of *Phellinotus piptadeniae* as revealed by phylogenomics

Our phylogenomic analysis placed *Phellinotus piptadeniae* in a strongly supported clade of closely related genera and species including *Sanghuanporus*, *Inonotus,* and *Phellinus igniarius*, all of which are wood-decay fungi with medicinal applications (21, 22), and *Fomitiporia mediterranea*, a broad-range trunk pathogen affecting grapevines (23), citrus (24), and olives (25) (Fig. 2 and 3). Although assembly and annotation metrics fit the variability found in Hymenochaetales (Fig. 3), *P. piptadeniae* differs from the other species for its narrow host specificity, considering its preference for *P. gonoacantha* and its limitation to other legume trees. Even though a close relationship of *P. piptadeniae* with those hymenomycetous genera was previously suggested based on a few genomic regions (15), their strong relatedness and divergence date based on genomic-wide data had not been estimated before. Our analysis obtained a single MRCA for these species around 2 Mya (Fig. 2).

This study presents new information about the origins of *P. piptadeniae*; however, we highlight the large gap of complete genomes available for this analysis. A previous phylogenetic study based on a concatenated set of genomic regions (15) mentioned several other genera (e.g., *Fomitiporella*, *Inocutis*, and *Fulviformes*) as closer to *P. piptadeniae* than *Sanghuangporus*. Unfortunately, none of those genera have assembled genomes available in public databases. The addition of such genomes could provide a better resolution in understanding which genes are in fact part of the "cloud" genome of *P.* piptadeniae (Fig. 4; Table S4 [available at https://github.com/LBMCF/phepip_isotopes]). The closeness of *P. piptadeniae* to species on the edge of saprotrophy and pathogenic lifestyles lays the basis for our working hypothesis. While *P. piptadeniae*

is strongly associated with living *P. gonoacantha* trees with no apparent pathogenic symptoms, could it be associated with a biotrophic lifestyle? Altogether, our results indicate that this is possible.

Several Hymenochaetaceae macrofungi are known to be tree pathogens, such as *Porodeaedalea pini* (Brot.) Murrill and *Phellinus tremulae* (Bondartsev) Bondartsev & P.N. Borisov, including species phylogenetically related to *P. piptadeniae* [such as *Fulvifomes fastuosus* (Lév.) Bondartseva & S. Herrera and *Tropicoporus linteus* (Berk. & M.A. Curtis) L.W. Zhou & Y.C. Dai] and a congeneric species [*Phellinotus badius* (Cooke) Salvador-Mont., Popoff & Drechsler-Santos] (11). These species, however, are usually pointed out to degrade the heartwood (dead organic matter within living trees), which could be a reason to classify them as saprotrophic. The work by (26) reports this saprotrophic and biotrophic lifestyle plasticity in other wood-decay basidiomycetes, which could lay the ground for understanding the trophic mode for *P. piptadeniae* and related species. Nonetheless, the aforementioned study concentrates on the plasticity of ectomycorrhizal species, which are generally contained in different clusters from *P. piptadeniae* in our stable isotope analysis, showing an opportunity for further studies in this matter.

Stable isotope analysis and CAZy content jointly suggest a pathotrophic lifestyle in *P. piptadeniae*

Conversely expected, considering the lignicolous habit of *P. piptadeniae* and previous results regarding the trophic modes of lignicolous fungi based on data from stable isotopes (9), our clustering analysis based on stable isotope data of *P. piptadeniae* and other species placed it outside the cluster that includes the vast majority of saprotrophic fungi (Fig. 5C and E; Tables S5 and S6 [available at https://github.com/LBMCF/phepip_isotopes]). Bioinformatics analyses based on the content of enzymes related to C metabolism also indicate a dichotomy in its feeding strategy, as well as other species in the order (Fig. 5F and 6; Table S7 [see at https://github.com/LBMCF/phepip_isotopes]).

Although the approach of radiocarbon isotopes (27) and stable isotopes have been mainly used for separating mycorrhizal fungi from saprotrophs (7), different outcomes have also been reported. For instance, the assemblage retrieved by Korotkin et al. (9) includes clusters containing a miscellaneous assemblage without a clear dominance of any specific trophic mode (including saprotrophs, ectomycorrhizal, and putative parasites or endophytes), which is where the majority of *P. piptadeniae* samples are located, when we added our data to their compilation (Fig. 5C through E). Furthermore, *P. piptadeniae* samples in this cluster share similar C ratio signatures as ECM, NS-NE, and bryophilous Hymenochaetales groups. On the other hand, their N ratio signatures are significantly different compared to ECM and NS-NE taxa but similar to saprotrophs and bryophilous Hymenochaetales. Korotkin et al. (9) observed a similar pattern for some bryophilous Hymenochaetales, speculating that they might obtain their carbon directly from their photosynthetic host. A recent and extensive study on different species of the wood saprotrophic genus *Mycena* (Basidiomycota, Agaricales) in distinct biomes and with several tree species indicated that *Mycena* spp. are also opportunist-generalist plant root invaders (28). Moreover, the aforementioned authors indeed emphasized that the conventional and widely used strict separation of macrofungi into the rigid ecological categories of mutualist, parasite/pathogen, or saprotroph has been frequently questioned, as reported in a study encompassing data from microcosm tests with 201 species of wood-decay searching for facultative biotrophy in saprotrophic basidiomycotan fungi (26). Although this evidence (Fig. 5 and 6,) points toward a non-saprotrophic trophic mode for *P. piptadeniae*, it is worth noting that distinct samples of the same species may group in different clusters in the stable isotope approach, putatively indicating distinct trophic modes. Nonetheless, this might be due to plasticity of carbon sources within that species (e.g., different samples with different habits), as previously investigated for distinct basidiomycotan saprotrophic macrofungi using combined carbon and nitrogen concentrations, isotopic ratios (^{13}C:^{12}C, ^{15}N:^{14}N, and ^{14}C:^{12}C), and compositional patterns in wood, cellulose, and basidiomata (29).

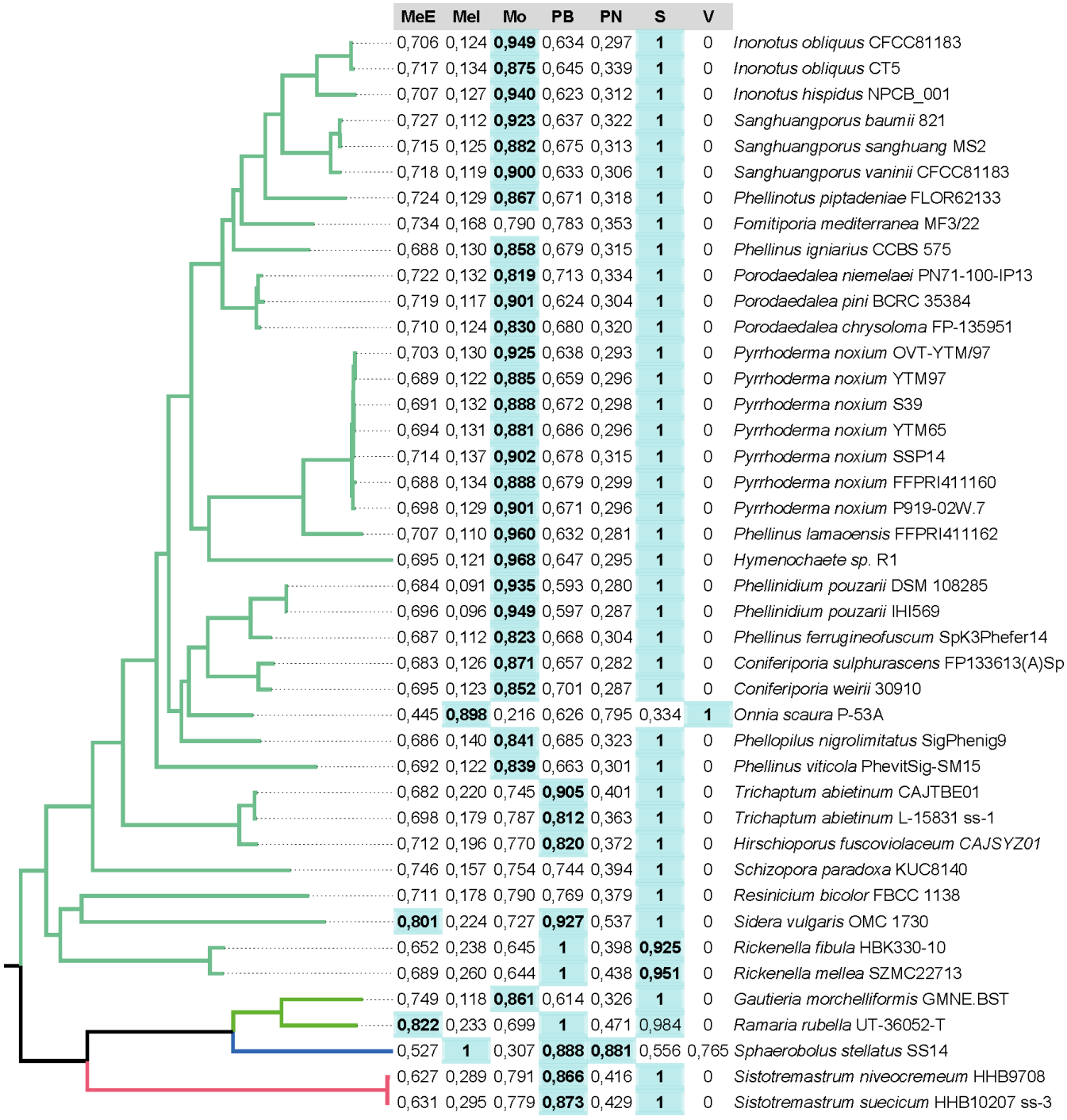

MeE	Mel	Mo	PB	PN	S	V	
0,706	0,124	**0,949**	0,634	0,297	**1**	0	*Inonotus obliquus* CFCC81183
0,717	0,134	**0,875**	0,645	0,339	**1**	0	*Inonotus obliquus* CT5
0,707	0,127	**0,940**	0,623	0,312	**1**	0	*Inonotus hispidus* NPCB_001
0,727	0,112	**0,923**	0,637	0,322	**1**	0	*Sanghuangporus baumii* 821
0,715	0,125	**0,882**	0,675	0,313	**1**	0	*Sanghuangporus sanghuang* MS2
0,718	0,119	**0,900**	0,633	0,306	**1**	0	*Sanghuangporus vaninii* CFCC81183
0,724	0,129	**0,867**	0,671	0,318	**1**	0	*Phellinotus piptadeniae* FLOR62133
0,734	0,168	0,790	0,783	0,353	**1**	0	*Fomitiporia mediterranea* MF3/22
0,688	0,130	**0,858**	0,679	0,315	**1**	0	*Phellinus igniarius* CCBS 575
0,722	0,132	**0,819**	0,713	0,334	**1**	0	*Porodaedalea niemelaei* PN71-100-IP13
0,719	0,117	**0,901**	0,624	0,304	**1**	0	*Porodaedalea pini* BCRC 35384
0,710	0,124	**0,830**	0,680	0,320	**1**	0	*Porodaedalea chrysoloma* FP-135951
0,703	0,130	**0,925**	0,638	0,293	**1**	0	*Pyrrhoderma noxium* OVT-YTM/97
0,689	0,122	**0,885**	0,659	0,296	**1**	0	*Pyrrhoderma noxium* YTM97
0,691	0,132	**0,888**	0,672	0,298	**1**	0	*Pyrrhoderma noxium* S39
0,694	0,131	**0,881**	0,686	0,296	**1**	0	*Pyrrhoderma noxium* YTM65
0,714	0,137	**0,902**	0,678	0,315	**1**	0	*Pyrrhoderma noxium* SSP14
0,688	0,134	**0,888**	0,679	0,299	**1**	0	*Pyrrhoderma noxium* FFPRI411160
0,698	0,129	**0,901**	0,671	0,296	**1**	0	*Pyrrhoderma noxium* P919-02W.7
0,707	0,110	**0,960**	0,632	0,281	**1**	0	*Phellinus lamaoensis* FFPRI411162
0,695	0,121	**0,968**	0,647	0,295	**1**	0	*Hymenochaete sp.* R1
0,684	0,091	**0,935**	0,593	0,280	**1**	0	*Phellinidium pouzarii* DSM 108285
0,696	0,096	**0,949**	0,597	0,287	**1**	0	*Phellinidium pouzarii* IHI569
0,687	0,112	**0,823**	0,668	0,304	**1**	0	*Phellinus ferrugineofuscum* SpK3Phefer14
0,683	0,126	**0,871**	0,657	0,282	**1**	0	*Coniferiporia sulphurascens* FP133613(A)Sp
0,695	0,123	**0,852**	0,701	0,287	**1**	0	*Coniferiporia weirii* 30910
0,445	**0,898**	0,216	0,626	0,795	0,334	**1**	*Onnia scaura* P-53A
0,686	0,140	**0,841**	0,685	0,323	**1**	0	*Phellopilus nigrolimitatus* SigPhenig9
0,692	0,122	**0,839**	0,663	0,301	**1**	0	*Phellinus viticola* PhevitSig-SM15
0,682	0,220	0,745	**0,905**	0,401	**1**	0	*Trichaptum abietinum* CAJTBE01
0,698	0,179	0,787	**0,812**	0,363	**1**	0	*Trichaptum abietinum* L-15831 ss-1
0,712	0,196	0,770	**0,820**	0,372	**1**	0	*Hirschioporus fuscoviolaceum CAJSYZ01*
0,746	0,157	0,754	0,744	0,394	**1**	0	*Schizopora paradoxa* KUC8140
0,711	0,178	0,790	0,769	0,379	**1**	0	*Resinicium bicolor* FBCC 1138
0,801	0,224	0,727	**0,927**	0,537	**1**	0	*Sidera vulgaris* OMC 1730
0,652	0,238	0,645	**1**	0,398	**0,925**	0	*Rickenella fibula* HBK330-10
0,689	0,260	0,644	**1**	0,438	**0,951**	0	*Rickenella mellea* SZMC22713
0,749	0,118	**0,861**	0,614	0,326	**1**	0	*Gautieria morchelliformis* GMNE.BST
0,822	0,233	0,699	**1**	0,471	0,984	0	*Ramaria rubella* UT-36052-T
0,527	**1**	0,307	**0,888**	**0,881**	0,556	0,765	*Sphaerobolus stellatus* SS14
0,627	0,289	0,791	**0,866**	0,416	**1**	0	*Sistotremastrum niveocremeum* HHB9708
0,631	0,295	0,779	**0,873**	0,429	**1**	0	*Sistotremastrum suecicum* HHB10207 ss-3

FIG 6 Trophic mode scores based on the CAZy profile. Scores higher than 0.8 are highlighted in bold and green background. MeE = Extracellular mesotrophs, Mel = Intracelullar mesotrophs, Mo = Monomertroph, PB = Broad host-range polymertrophs, PN = Narrow host-range polymertrophs, S = Saprotroph, and V = Vasculartrop.

Based on field observation of wood decomposition, it has been previously known that some Hymenochaetaceae plant pathogens are capable of degrading the sapwood from living trees (2, 11). Furthermore, *Ganoderma sessile* (Ganodermataceae, Polyporales) had already been experimentally inoculated in young trees (which possess only sapwood) of pine and oak and, around 1 year later, reisolated outside of the inoculation point, indicating the capacity to infect living sapwood (30). *Phellinotus piptadeniae* fruiting bodies are commonly found on high branches of *Piptadenia gonoacantha* but

rarely on the main trunk (Fig. 1C and D). Those branches likely exhibit poorly differentiated heartwood. Therefore, we hypothesize that *P. piptadeniae* might infect the living sapwood of *P. gonoacantha*, acquiring carbon from the living part of its host, explaining the pattern observed in our combined genomic stable isotope analysis.

MATERIAL AND METHODS

Phellinotus piptadeniae basidiomata occurrence and host association

The occurrence of the fungal species *Phellinotus piptadeniae* on living and dead host plants, its range and geographic distribution were obtained and confirmed from previously published systematic and biogeographic studies (14, 16), as well as from online databases (GBIF, https://www.gbif.org/; speciesLink, https://specieslink.net/; and MyCoPortal, https://www.mycoportal.org/portal/). A total of 80 taxonomically verified georeferenced herbarium collections of *P. piptadeniae* were assembled from the FLOR, IAC, HUEM, URM, and MVHC herbaria (Table S1 [available at https://github.com/LBMCF/phepip_isotopes]).

From the latitude and longitude of each collection, we extracted the monthly precipitation, and minimum and maximum temperatures using the WorldClim v.2.0 model layers (17) and the R package *raster* (31). The bioclimatic variables BIO12 (Annual Precipitation) and BIO15 (Coefficient of Variation of the Precipitation Seasonality) were derived from these climate models using the *extract* function of *raster*. We mapped the entire range distribution of *Phellinotus piptadeniae* against the BIO12 bioclimatic variable, using the R packages *raster*, *ggplot2* (32), *ggspatial* (33), and *rnaturalearth* (34). The bioclimatic space of *P. piptadeniae* was also assessed with a scatterplot that shows its distribution in different Brazilian phytogeographic domains and across the BIO12 and BIO15 axes.

For morphological and downstream genomic analyses, dehydrated basidiomata from a newly collected specimen of *P. piptadeniae* was obtained from a living tree of *Piptadenia gonoacantha* in the Atlantic Rainforest of southern Brazil (Parque do Córrego Grande, Florianópolis, State of Santa Catarina; Latitude: 27.599814 W, Longitude: 48.511375 S) and deposited at the FLOR fungarium under the voucher number FLOR62133. Macromorphological and micromorphological studies of collected basidiomata were made for fungal identification. For mycelium isolation, a piece from the collected fruiting body was removed and had its surface disinfected using 70% alcohol and distilled water, and subsequently inoculated in a 90 mm Petri dish containing MEA culture medium (2% malt extract, 2% glucose, and 2% agarose) supplemented with chloramphenicol. The Petri dish was incubated at 28 ± 2°C for 10 days and the fungal growth was daily checked.

Genomic DNA extraction and sequencing

Phellinotus piptadeniae CCMB738 was inoculated in MEA culture medium and incubated at 28 ± 2°C for 10 days. After growth, the mycelium was removed from the Petri dish. The total DNA was extracted using the FastDNA Spin Kit (MP Biomedicals, Irvine, California, USA) for sequencing on the HiSeq 2500 platform (Illumina, San Diego, California, USA) and the ZymoBIOMICS DNA Miniprep Kit (Zymo Research, Irvine, California, USA) for sequencing on the MinION platform (Oxford Nanopore Technologies, Oxford, UK). DNA was evaluated qualitatively in 1% agarose gel and quantitatively by Nanodrop 1000 ND spectrophotometer (Thermo Scientific, Waltham, Massachussetts, USA) and Qubit fluorometer (Invitrogen, Waltham, Massachussetts, USA). Paired-end sequencing on the HiSeq 2500 platform was carried out from 1 µg of DNA, using the NEBNext Fast DNA Fragmentation and Library Preparation Kit (New England Biolabs, Ipswich, Massachusetts, USA). For MinION sequencing, genomic DNA was fragmented to 8 Kbp using the Covaris g-TUBE (Covaris, Woburn, Massachussetts, USA) and purified using AMPureXP beads reagent (Beckman Coulter Inc., Brea, California, USA). Subsequently, the library was prepared following the protocol described by Tomé et al. (35) and sequenced for 24 hours using the MinKNOW software with real-time base calling.

Raw data processing, *de novo* genome assembly, and annotation

Raw reads from the Illumina platform were evaluated for quality using FastQC v0.11.5 software (36). Subsequently, the bases with a Phred score equal to or less than 20 were trimmed using the BBDuk software (37). The raw reads obtained through MinION sequencing were demultiplexed and had the adapters trimmed using the Porechop software (38). The *P. piptadeniae* genome was assembled using the *de novo* approach and the MaSuRCA-Purge_dups hybrid assembly pipeline, described by Tomé et al. (35). This assembly workflow uses the MaSuRCA software to generate a primary assembly from both short-reads (HiSeq 2500) and long-reads (MinION), and the Purge_Dups program to identify and remove haplotypic duplications (39, 40). The generated genome was evaluated for length, largest contig size, N50, and L50 metrics, using QUAST v4.6.0 software (41). The BUSCO v4 software (Benchmarking Universal Single-Copy Orthologs) was used to verify the completeness of single-copy orthologous genes (42). For this analysis, the basidiomycota_odb10 database was used.

Genome annotation was carried out using the Funannotate pipeline v1.8.17 (43), using 114030 proteins and 12293 ESTs from Hymenochaetales as evidence. Briefly, transcript evidence (ESTs) was aligned to the genome using minimap2 (44), while protein sequences were aligned using Diamond/Exonerate (45, 46). Conserved orthologs were identified with BUSCO (42), and the gene prediction was performed using GeneMark-ES (47), Augustus (48), SNAP (49), Glimmer HMM (50), and EVidenceModeler (51). The tRNA genes were predicted using tRNAscan-SE (52).

Prediction of carbohydrate-active enzymes

The carbohydrate-active enzymes (CAZy) were identified from the predicted proteins file, either from Funannotate pipeline v1.8.17 (43) or from GenBank and JGI using the Catastrophy software v0.1.0 (19). Catastrophy uses CAZy predictions from HMMER (53) to infer lifestyle in plant-infecting fungi.

Comparative genomics, phylogenomics, and homology assignment

Homology assignment of gene families was performed using OrthoFinder v2.5.2 (54). The taxon sampling in this analysis comprises *P. piptadeniae* and 41 other species of Hymenochaetales, Trechisporales, Gomphales, and Geastrales (the species from the latter three orders as outgroup) for which public genomes were available (Table S2; available at https://github.com/LBMCF/phepip_isotopes). The species-level phylogenomic tree was inferred using 1,123 single-copy orthologous gene families whose proteins were aligned using the built-in MAFFT module in OrthoFinder with default parameters and then concatenated in a supermatrix. We used IQ-TREE v. 2.1.2 (55) for phylogenomic inference with the parameter "-m TEST" to calculate the best fitting model using BIC criteria, which was JTT + F + I + G4, with 1,000 ultra-fast bootstrap replicates for branch support. IQ-TREE was also used for the time calibration of the tree with the least-squares analysis and two calibration points obtained from the TimeTree database (56): 243 Mya for the most recent common ancestor (MRCA) of *Hymenochaetales* and *Trechisporales*, and 2.003 Mya for the MRCA of *Phellinus igniarius* (L.) Quél. and *Fomitiporia mediterranea* M. Fisch.

Stable isotope analysis

The carbon and nitrogen isotope ratios were determined by combustion using an elemental analyzer (Carlo Erba, CHN-1100) coupled to a Thermo Finnigan Delta Plus mass spectrometer at the Laboratory of Isotope Ecology of the Centro de Energia Nuclear na Agricultura (CENA/Universidade de São Paulo), in Piracicaba, State of São Paulo, Brazil. Isotope ratios are reported in per mil (‰), where $\delta^{13}C$ is reported relative to the Vienna Pee Dee Belemnite (VPDB; ^{13}C:^{12}C ratio = 0.01118) standard and $\delta^{15}N$ is reported relative to atmospheric air (AIR; ^{15}N:^{14}N ratio = 0.0036765). Internal standards (sugarcane leaves) are routinely interspersed with target samples to correct for mass effects and instrumental drift during and between runs. Long-term analytical error for the internal standards

was 0.2‰ for both $\delta^{13}C$ and $\delta^{15}N$, 1% for organic C, and 0.02% for total N. The carbon and nitrogen isotope ratios of field-collected samples of *P. piptadeniae*, and leaf samples from *P. gonoacantha* were determined by combustion using an elemental analyzer coupled to a mass spectrometer.

The samples generated in this study were added to the compilation provided by Korotkin et al. (9) and their clustering analysis was repeated. Briefly, $\delta^{13}C$ and $\delta^{15}N$ values were clustered with the *Mclust* package in R (57). The three fitting models presented by Korotkin were replicated: VVV with three components, VEV, and VVI both with four components. The categories set by the authors were saprotrophic (SAP), ectomycorrhizal (ECM), neither saprotrophic nor ectomycorrhizal (NS-NE), bryophilous Hymenochaetales (their test data set), and *Dicranum scoparium* Hedw. samples as a positive control for autotrophs. We tested the data for normality (values of $\delta^{13}C$ and $\delta^{15}N$) to decide the application of one-way ANOVA or the Kruskal-Wallis test (58) to test the difference between the groups recovered in the best-fit model of *Mclust* analysis. As the data did not exhibit a normal distribution, we applied the Kruskal-Wallis test following the application of Dunn's test (59) for testing for differences between each pair of recovered groups. Similarly, we applied the same tests to test the null hypothesis of no differences between *P. piptadeniae* values of $\delta^{13}C$ and $\delta^{15}N$ and trophic groups (SAP, ECM, NS-NE, AUTO, and bryophilous Hymenochaetales) recovered in the same cluster (considering the best-fit model). Tests were performed in R with in-house functions and the *dunn.test* package (60).

ACKNOWLEDGMENTS

We are grateful to the 1,000 Fungal Genomes project consortium, especially Dr. Francis Martin, Dr. Otto Miettinen, and Dr. Sundy Maurice for granting access to unpublished genome data. The genome sequence data were produced by the US Department of Energy Joint Genome Institute in collaboration with the user community. E.R.D.-S., A.G.-N., and D.C. are supported by Research Productivity Scholarships from Conselho Nacional de Desenvolvimento Científico e Tecnológico (CNPq) (Grants 310150/2022–1, 308880/2022–6, and 314187/2021–9, respectively). L.M.R.T. received a Postdoctoral Scholarship (Process number: 152665/2022-6) from CNPq. The authors declare that they have no competing interests.

E.R.D.-S., A.G.-N., L.M.R.T., and G.Q.-P. conceived and designed the experiments. All authors analyzed the data. L.M.R.T. and D.S.A. prepared biological material and performed the wet bench experiments. L.M.R.T., G.Q-P., D.H.C-R., C.A.S-M., and D.C. conducted the bioinformatic analysis. J.M.F. and G.B.N. conducted the stable isotope analyses. L.M.R.T., G.Q-P., D.H.C-R., C.A.S.-M., D.C., G.A.-S., E.R.D.-S., and A.G.-N. wrote the original draft.

We greatly thank Dr. Erik Hobbie for his excellent and insightful review, as well as an anonymous reviewer for his superb and highly detailed review. Their reviews were fundamental for the greatly improving our paper!

AUTHOR AFFILIATIONS

[1]Department of Microbiology, Molecular and Computational Biology of Fungi Laboratory, Instituto de Ciências Biológicas, Universidade Federal de Minas Gerais, Belo Horizonte, Brazil
[2]Departamento de Ciências Biológicas, Programa de Pós-graduação em Botânica, Universidade Estadual de Feira de Santana, Feira de Santana, Brazil
[3]MIND.Funga (Monitoring and Inventorying Neotropical Diversity of Fungi) - MICOLAB, Universidade Federal de Santa Catarina, Florianópolis, Brazil
[4]Fundación Miguel Lillo, Instituto Criptogámico-Sección Micología, San Miguel de Tucumán, Argentina
[5]Organización Juvenil "Hongos Perú", Cusco, Santiago, Peru
[6]Instituto de Pesquisas Jardim Botânico do Rio de Janeiro (JBRJ), Rio de Janeiro, Brazil

[7]Instituto de Biologia, Universidade Federal da Bahia, Salvador, Brazil
[8]Program in Bioinformatics, Loyola University Chicago, Chicago, Illinois, USA
[9]Departamento de Ecologia, Universidade de Brasília, Brasília, Brazil

AUTHOR ORCIDs

Luiz Marcelo Ribeiro Tomé http://orcid.org/0000-0002-1477-5558
Aristóteles Góes-Neto http://orcid.org/0000-0002-7692-6243

FUNDING

Funder	Grant(s)	Author(s)
Conselho Nacional de Desenvolvimento Científico e Tecnológico (CNPq)	310150/2022-1	Elisandro Ricardo Drechsler-Santos
Conselho Nacional de Desenvolvimento Científico e Tecnológico (CNPq)	308880/2022-6	Aristóteles Góes-Neto
Conselho Nacional de Desenvolvimento Científico e Tecnológico (CNPq)	314187/2021-9	Domingos Cardoso

AUTHOR CONTRIBUTIONS

Luiz Marcelo Ribeiro Tomé, Data curation, Formal analysis, Investigation, Methodology, Validation, Writing – original draft, Writing – review and editing | Gabriel Quintanilha-Peixoto, Conceptualization, Data curation, Formal analysis, Investigation, Methodology, Writing – original draft, Writing – review and editing | Diogo Henrique Costa-Rezende, Data curation, Formal analysis, Investigation, Writing – original draft, Writing – review and editing | Carlos A. Salvador-Montoya, Data curation, Formal analysis, Investigation, Writing – original draft, Writing – review and editing | Domingos Cardoso, Data curation, Formal analysis, Investigation, Writing – original draft, Writing – review and editing | Daniel S. Araújo, Data curation, Formal analysis | Jorge Marcelo Freitas, Investigation, Methodology, Resources | Gabriela Bielefeld Nardoto, Formal analysis, Investigation, Methodology, Resources | Elisandro Ricardo Drechsler-Santos, Conceptualization, Funding acquisition, Investigation, Project administration, Resources, Writing – original draft, Writing – review and editing | Aristóteles Góes-Neto, Conceptualization, Formal analysis, Funding acquisition, Investigation, Project administration, Supervision, Writing – original draft, Writing – review and editing.

DATA AVAILABILITY

All Supplementary Tables and Figures are available at the GitHub repository of this study (https://github.com/LBMCF/phepip_isotopes).

REFERENCES

1. Moore D, Robson GD, Trinci APJ. 2011. *21st century guidebook to fungi*. Cambridge, UK.
2. Hennon PE. 1995. Are heart rot fungi major factors of disturbance in gap-dynamic forests? Northwest Sci 69:284–293.
3. Hibbett DS, Stajich JE, Spatafora JW. 2013. Toward genome-enabled mycology. Mycologia 105:1339–1349. https://doi.org/10.3852/13-196
4. Zhao Z, Liu H, Wang C, Xu JR. 2013. Comparative analysis of fungal genomes reveals different plant cell wall degrading capacity in fungi. BMC Genomics 14:274. https://doi.org/10.1186/1471-2164-14-274
5. Sista Kameshwar AK, Qin W. 2018. Comparative study of genome-wide plant biomass-degrading cazymes in white rot, brown rot and soft rot fungi. Mycology 9:93–105. https://doi.org/10.1080/21501203.2017.1419296
6. Larsen T, Taylor DL, Leigh MB, O'Brien DM. 2009. Stable isotope fingerprinting: a novel method for identifying plant, fungal, or bacterial origins of amino acids. Ecology 90:3526–3535. https://doi.org/10.1890/08-1695.1
7. Mayor JR, Schuur EAG, Henkel TW. 2009. Elucidating the nutritional dynamics of fungi using stable isotopes. Ecol Lett 12:171–183. https://doi.org/10.1111/j.1461-0248.2008.01265.x
8. Tedersoo L, Naadel T, Bahram M, Pritsch K, Buegger F, Leal M, Kõljalg U, Põldmaa K. 2012. Enzymatic activities and stable isotope patterns of ectomycorrhizal fungi in relation to phylogeny and exploration types in an afrotropical rain forest. New Phytol 195:832–843. https://doi.org/10.1111/j.1469-8137.2012.04217.x
9. Korotkin HB, Swenie RA, Miettinen O, Budke JM, Chen K-H, Lutzoni F, Smith ME, Matheny PB. 2018. Stable isotope analyses reveal previously unknown trophic mode diversity in the Hymenochaetales. Am J Bot 105:1869–1887. https://doi.org/10.1002/ajb2.1183
10. Larsson K-H, Parmasto E, Fischer M, Langer E, Nakasone KK, Redhead SA. 2006. Hymenochaetales: a molecular phylogeny for the hymenochaetoid clade. Mycologia 98:926–936. https://doi.org/10.3852/mycologia.98.6.926
11. Cibrián-Tova D, Alvarado Rosales D, García Díaz SE. 2007. Forest diseases in Mexico

12. Dai YC, Cui BK, Yuan HS, Li BD. 2007. Pathogenic wood-decaying fungi in China. Forest Path 37:105–120. https://doi.org/10.1111/j.1439-0329.2007.00485.x
13. Salvador-Montoya C. A., Robledo GL, Cardoso D, Borba-Silva MA, Fernandes M, Drechsler-Santos ER. 2015. Phellinus piptadeniae (Hymenochaetales: Hymenochaetaceae): taxonomy and host range of a species with disjunct distribution in South American seasonally dry forests. Plant Syst Evol 301:1887–1896. https://doi.org/10.1007/s00606-015-1201-6
14. Salvador-Montoya Carlos A., Elias SG, Popoff OF, Robledo GL, Urcelay C, Góes-Neto A, Martínez S, Drechsler-Santos ER. 2022. Neotropical studies on Hymenochaetaceae: unveiling the diversity and endemicity of phellinotus. JoF 8:216. https://doi.org/10.3390/jof8030216
15. Drechsler-santos ER, Robledo GL, Lima-júnior NC, Malosso E, Reck MA, Gibertoni TB, Cavalcanti MADQ, Rajchenberg M. 2016. "Phellinotus, a new neotropical genus in the Hymenochaetaceae (Basidiomycota, Hymenochaetales),". Phytotaxa 261:218. https://doi.org/10.11646/phytotaxa.261.3.2
16. Elias SG, Salvador-Montoya CA, Costa-Rezende DH, Guterres DC, Fernandes M, Olkoski D, Klabunde GHF, Drechsler-Santos ER. 2020. Studies on the biogeography of phellinotus piptadeniae (Hymenochaetales, Basidiomycota): expanding the knowledge on its distribution and clarifying hosts relationships. Fun Ecol 45:100912. https://doi.org/10.1016/j.funeco.2020.100912
17. Fick SE, Hijmans RJ. 2017. WorldClim 2: new 1-km spatial resolution climate surfaces for global land areas. Intl J Clim 37:4302–4315. https://doi.org/10.1002/joc.5086
18. Petersen C, Sørensen T, Nielsen MR, Sondergaard TE, Sørensen JL, Fitzpatrick DA, Frisvad JC, Nielsen KL. 2023. "Comparative genomic study of the penicillium genus elucidates a diverse pangenome and 15 lateral gene transfer events,". IMA Fungus 14:3. https://doi.org/10.1186/s43008-023-00108-7
19. Hane JK, Paxman J, Jones DAB, Oliver RP, de Wit P. 2019. "'CATAStrophy,' a genome-informed trophic classification of filamentous plant pathogens – how many different types of filamentous plant pathogens are there?". Front Microbiol 10:3088. https://doi.org/10.3389/fmicb.2019.03088
20. Särkinen T, Iganci JRV, Linares-Palomino R, Simon MF, Prado DE. 2011. Forgotten forests - issues and prospects in biome mapping using seasonally dry tropical forests as a case study. BMC Ecol 11:vember. https://doi.org/10.1186/1472-6785-11-27
21. Lee S, Kim JI, Heo J, Lee I, Park S, Hwang M-W, Bae J-Y, Park MS, Park HJ, Park M-S. 2013. The anti-influenza virus effect of phellinus igniarius extract. J Microbiol 51:676–681. https://doi.org/10.1007/s12275-013-3384-2
22. Jiang JH, Wu SH, Zhou LW. 2021. The first whole genome sequencing of *Sanghuangporus sanghuang* provides insights into its medicinal application and evolution. JoF 7:787. https://doi.org/10.3390/jof7100787
23. Bruno GL, Ippolito MP, Mannerucci F, Bragazzi L, Tommasi F. 2021. "Physiological responses of 'Italia' grapevines infected with ESCA pathogens". Phytopathol Mediterr 60:321–336. https://doi.org/10.36253/phyto-12171
24. Elena K, Fischer M, Dimou D, Dimou DM. 2006. Fomitiporia mediterranea infecting citrus trees in Greece. Phytopathol Mediterr 45:35–39.
25. Markakis EA, Ligoxigakis EK, Roussos PA, Sergentani CK, Kavroulakis N, Roditakis EN, Koubouris GC. 2019. Differential susceptibility responses of greek olive cultivars to *Fomitiporia mediterranea*. Eur J Plant Pathol 153:1055–1066. https://doi.org/10.1007/s10658-018-01622-w
26. Smith GR, Finlay RD, Stenlid J, Vasaitis R, Menkis A. 2017. Growing evidence for facultative biotrophy in saprotrophic fungi: data from microcosm tests with 201 species of wood-decay basidiomycetes. New Phytol 215:747–755. https://doi.org/10.1111/nph.14551
27. Hobbie Erik A., Weber NS, Trappe JM, Van Klinken GJ. 2002. Using radiocarbon to determine the mycorrhizal status of fungi. New Phy 156:129–136. https://doi.org/10.1046/j.1469-8137.2002.00496.x
28. Harder CB, Hesling E, Botnen SS, Lorberau KE, Dima B, von Bonsdorff-Salminen T, Niskanen T, Jarvis SG, Ouimette A, Hester A, Hobbie EA, Taylor AFS, Kauserud H. 2023. Mycena species can be opportunist-generalist plant root invaders. Environ Microbiol 25:1875–1893. https://doi.org/10.1111/1462-2920.16398
29. Hobbie E. A., Grandy AS, Harmon ME. 2020. Isotopic and compositional evidence for carbon and nitrogen dynamics during wood decomposition by saprotrophic fungi. Fun Ecol 45:100915. https://doi.org/10.1016/j.funeco.2020.100915
30. Loyd AL, Linder ER, Anger NA, Richter BS, Blanchette RA, Smith JA. 2018. Pathogenicity of ganoderma species on landscape trees in the southeastern United States. Plant Dis 102:1944–1949. https://doi.org/10.1094/PDIS-02-18-0338-RE
31. Hijmans RJ, van Etten J. 2012. raster: geographic analysis and modeling with raster data. R package version 2.0-12
32. Wickham H. 2016. ggplot2: create elegant data visualisations using the grammar of graphics. R package version 3.2. 1. In Stata Softw Packag Coll station. TX, USA.
33. Dunnington D, Thorne B. 2020. ggspatial: spatial data framework for ggplot2. R Packag. version. Vol. 1.
34. South A. 2017. Rnaturalearth: world map data from natural earth. R Packag. version 0.1.0
35. Tomé LMR, da Silva FF, Fonseca PLC, Mendes-Pereira T, Azevedo VA de C, Brenig B, Badotti F, Góes-Neto A. 2022. Hybrid assembly improves genome quality and completeness of *Trametes villosa* CCMB561 and reveals a huge potential for lignocellulose breakdown. JoF 8:142. https://doi.org/10.3390/jof8020142
36. S. Andrews, "FastQC: a quality control tool for high throughput sequence data." Babraham Bioinformatics, Babraham Institute, Cambridge, United Kingdom, 2010.
37. Bushnell B. 2018. Bbtools: a suite of fast, multithreaded bioinformatics tools designed for analysis of DNA and RNA sequence data. Jt. Genome Institute. Available from: https//jgi. doe. gov/data-and-tools/bbtools
38. Wick R, Volkening J, Loman N. 2017. Porechop
39. Zimin AV, Marçais G, Puiu D, Roberts M, Salzberg SL, Yorke JA. 2013. The masurca genome assembler. Bioinformatics 29:2669–2677. https://doi.org/10.1093/bioinformatics/btt476
40. Guan D, McCarthy SA, Wood J, Howe K, Wang Y, Durbin R. 2020. Identifying and removing haplotypic duplication in primary genome assemblies. Bioinformatics 36:2896–2898. https://doi.org/10.1093/bioinformatics/btaa025
41. Gurevich A, Saveliev V, Vyahhi N, Tesler G. 2013. QUAST: quality assessment tool for genome assemblies. Bioinformatics 29:1072–1075. https://doi.org/10.1093/bioinformatics/btt086
42. Simão FA, Waterhouse RM, Ioannidis P, Kriventseva EV, Zdobnov EM. 2015. BUSCO: assessing genome assembly and annotation completeness with single-copy orthologs. Bioinformatics 31:3210–3212. https://doi.org/10.1093/bioinformatics/btv351
43. Agudelo-Valencia D, Uribe-Echeverry PT, Betancur-Pérez JF. 2020. *De novo* assembly and annotation of the ganoderma australe genome. Genomics 112:930–933. https://doi.org/10.1016/j.ygeno.2019.06.008
44. Li H. 2018. Minimap2: pairwise alignment for nucleotide sequences. Bioinformatics 34:3094–3100. https://doi.org/10.1093/bioinformatics/bty191
45. Buchfink B, Xie C, Huson DH. 2015. Fast and sensitive protein alignment using DIAMOND. Nat Methods 12:59–60. https://doi.org/10.1038/nmeth.3176
46. Slater GSC, Birney E. 2005. Automated generation of heuristics for biological sequence comparison. BMC Bioinformatics 6:1–11. https://doi.org/10.1186/1471-2105-6-31
47. Brůna T, Lomsadze A, Borodovsky M. 2020. Genemark-EP+: eukaryotic gene prediction with self-training in the space of genes and proteins. NAR Gen Bioinform 2:1–14. https://doi.org/10.1093/nargab/lqaa026
48. Stanke M, Steinkamp R, Waack S, Morgenstern B. 2004. AUGUSTUS: a web server for gene finding in eukaryotes. Nucleic Acids Res 32:W309–12. https://doi.org/10.1093/nar/gkh379
49. Korf I. 2004. Gene finding in novel genomes. BMC Bioinformatics 5:1–9. https://doi.org/10.1186/1471-2105-5-59
50. Majoros WH, Pertea M, Salzberg SL. 2004. Tigrscan and GlimmerHMM: two open source ab initio eukaryotic gene-finders. Bioinformatics 20:2878–2879. https://doi.org/10.1093/bioinformatics/bth315
51. Haas BJ, Salzberg SL, Zhu W, Pertea M, Allen JE, Orvis J, White O, Buell CR, Wortman JR. 2008. Automated eukaryotic gene structure annotation using evidencemodeler and the program to assemble spliced

alignments. Genome Biol 9:1–22. https://doi.org/10.1186/gb-2008-9-1-r7
52. Chan PP, Lin BY, Mak AJ, Lowe TM. 2021. TRNAscan-SE 2.0: improved detection and functional classification of transfer RNA genes. Nucleic Acids Res 49:9077–9096. https://doi.org/10.1093/nar/gkab688
53. Potter SC, Luciani A, Eddy SR, Park Y, Lopez R, Finn RD. 2018. HMMER web server: 2018 update. Nucleic Acids Res 46:W200–W204. https://doi.org/10.1093/nar/gky448
54. Emms DM, Kelly S. 2018. OrthoFinder: phylogenetic orthology inference for comparative genomics. Bioinformatics. https://doi.org/10.1101/466201
55. Minh BQ, Schmidt HA, Chernomor O, Schrempf D, Woodhams MD, von Haeseler A, Lanfear R. 2020. IQ-TREE 2: new models and efficient methods for phylogenetic inference in the genomic era. Mol Biol Evol 37:1530–1534. https://doi.org/10.1093/molbev/msaa015
56. Kumar S, Stecher G, Suleski M, Hedges SB. 2017. Timetree: a resource for timelines, timetrees, and divergence times. Mol Biol Evol 34:1812–1819. https://doi.org/10.1093/molbev/msx116
57. Scrucca L, Fop M, Murphy BT, Raftery AE. 2016. Mclust. R J 8:289–317. https://doi.org/10.32614/RJ-2016-021
58. Kruskal WH, Wallis WA. 1952. Use of ranks in one-criterion variance analysis. J American Stat Association 47:583–621. https://doi.org/10.1080/01621459.1952.10483441
59. Dunn OJ. 1964. Multiple comparisons using rank sums. Technometrics 6:241–252. https://doi.org/10.1080/00401706.1964.10490181
60. Dinno A. 2017. Package 'Dunn.test. CRAN Repos:1–7. https://cran.r-project.org/web/packages/dunn.test/dunn.test.pdf.